Stark spectrum of barium in highly excited Rydberg states*

Yang Hai-Feng(杨海峰), Gao Wei(高 伟), Cheng Hong(成 红), Liu Xiao-Jun(柳晓军), and Liu Hong-Ping(刘红平)†

State Key Laboratory of Magnetic Resonance and Atomic and Molecular Physics, Wuhan Institute of Physics and Mathematics, Chinese Academy of Sciences, Wuhan 430071, *China*

(Received 17 May 2012; revised manuscript received 6 July 2012)

We present observations of Stark spectra of barium in highly excited Rydberg states in the energy region around $n = 35$. The one-photon excitation concerns the π transition. The observed Stark spectra at electric fields ranging from 0 to 60 V·cm^{-1} are well explained by the diagonalization of the Hamiltonian incorporating the core effects. From the Stark maps, the anti-crossings between energy levels are identified experimentally and theoretically. The time of flight spectra at the specified Stark states are recorded, where the deceleration and acceleration of barium atoms are observed. This is very consistent with the prediction derived from the Stark maps from the point of view of energy conservation.

Keywords: Stark effect, barium, time of flight

PACS: 32.60.+i, 32.30.–r, 82.80.Rt **DOI:** 10.1088/1674-1056/22/1/013202

1. Introduction

The study of spectroscopic properties of an atom in an external electric field, which is easily accessible experimentally, has been a subject of permanent interest for many years.[1] The general approach used to explore this system is to record the spectrum directly with a pulsed dye laser (with a linewidth of a few GHz) or a continuous wave laser (with a linewidth of tens of MHz),[2–4] rather than the scaled methods.[5,6] The studies of an atom in an electric field using a pulsed dye laser mainly focus on the Stark structure below[7,8] or above, the classical ionization threshold[9–11] and the ionization process.[12,13] Atomic species under investigation cover a wide range, including hydrogen,[14] alkali atoms,[8,15] earth alkali,[16,17] and noble gases.[18] Most Stark spectra below the classical ionization threshold are obtained from atoms with a principal quantum number below $n = 20$ and an electric field up to several kilovolts per centimeter. In this paper, the Stark spectra of barium with an energy around $n = 35$ and an electric field only tens of volts per centimeter are obtained, where the anti-crossings between levels are identified.

Theoretically, atoms in an electric field can be studied using the perturbation theory[1,15] and numerical calculations within a full quantum scheme.[17,19,20] $\boldsymbol{R}$-matrix based quantum defect theory is developed to include the core effect and applied to the Stark spectral calculation.[21] At the same time, an alternative method of quantum defect orbit is also applied to incorporate the quantum defects explicitly, usually called the "exact quantum defect theory".[22] This method can give analytical wavefunctions to yield the "exact" quantum-defect eigenvalues and eigenfunctions, which provides an appropriate basis for the Stark problem in an external electric field.[23] The alternative model potential in this method exhibits more direct physics for the quantum defect effects. To avoid optimizing the radial nodes for the wavefunctions of the quantum-defect eigenvalues, one can also expand the Schrödinger equation directly in some situations. In this paper, we will expand the radial wavefunction in the B-spline basis.

In an external inhomogeneous electric field, any dipole atom or molecule will experience a force. This property can been used to control the motion of an atom or molecule by constructing a suitable electric field gradient. This idea[24] was proposed 30 years ago, but it was only realized experimentally in the last ten years for deflection[25–27] or deceleration (acceleration).[28–30] The loss/gain in kinetic energy is equal to $\Delta E = 3nk\Delta F/2$ (k runs from $-(n-1-|m_l|)$ to $(n-1-|m_l|)$ in a step of two, with n being the principal quantum number, k the parabolic quantum number, and F the electric field strength). Considering the magnitude of the dipole moment of Rydberg atoms is proportional to n^2, the highly excited atoms are more easily handled with a moderate electric field. The stark deceleration of Rydberg atoms has been achieved in hydrogen[31] and argon.[32] By imposing a travelling electric-field gradient on the moving Rydberg atoms, people can cut down the kinetic energy by more than $3nk\Delta F/2$ and even trap the atoms.[33,34]

In this paper, we choose barium as our research object due to its suitable ionization threshold and interesting non-hydrogen effects, i.e., the core effects.[35,36] Since the Stark structure of barium is fairly complex, we acquire the Stark map experimentally in advance to affirm the property of different states. Theoretically, the Stark map can be calculated in the same energy range as our well-developed method.[36] With the Stark maps, we choose the Stark states with positive or negative dipole moments and record their time of flight (TOF) spectra, where the acceleration and deceleration can be

*Project supported by the National Natural Science Foundation of China (Grant Nos. 11174329 and 91121005) and the National Basic Research Program of China (Grant No. 2013CB922003).

†Corresponding author. E-mail: liuhongping@wipm.ac.cn

© 2013 Chinese Physical Society and IOP Publishing Ltd

observed. The electric fields are selected just below the anti-crossing value in order to simplify the analysis of the deceleration/acceleration.

2. Theory

In the presence of an electric field applied in the z direction, the Hamiltonian H for a barium atom can be written as follows (in atomic units):

$$H = \frac{p^2}{2} + V_{\rm r} + Fz, \tag{1}$$

where F is the electric field strength in an atomic unit, and $V_{\rm r}$ is the Coulomb potential considering the polarization effects of the atomic core. The term $V_{\rm r}$ deviates from the form of $-1/r$ at small values of r. The complexity of the core-induced electron screening makes the Schrödinger equation for the non-hydrogen centrifugal problem to be lost analyticity. In this case, the term $V_{\rm r}$ is usually expressed by the model potential, parameterized by some angular momentum-dependent variables, which are closely correlated with quantum defects. Rather than using the model potential $V_{\rm r}$[6,37] or the $\boldsymbol{R}$-Matrix method including the quantum defects implicitly,[21] we employ an equivalent form for the central field potential[22]

$$V_{\rm r} = \frac{\lambda(\lambda+1) - l(l+1)}{2r^2} - \frac{1}{r}, \tag{2}$$

where $\lambda = l - \delta + {\rm Int}(\delta)$ and the quantum defects are explicitly enclosed. Here ${\rm Int}(\delta)$ is the rounded nearest integer value of the quantum defect. We employ a reduced quantum defect

$$\delta' = \delta - {\rm Int}(\delta) \tag{3}$$

to quantify and describe the real contribution of the quantum defect for a given angular momentum channel. In the following text, we will use δ' rather than δ and ignore the prime.

Instead of using the second Whittaker functions as the basis,[38] which are called quantum defect orbits, making it possible to perform a multi-channel quantum defect theory (MQDT) based calculation, in the present work, we will take the B-spline function as the basis. In this basis, the Hamiltonian has a symmetric banded matrix form. This special matrix structure will save much time in numerical diagonalization to obtain the final eigenvalues and eigenfunctions. In addition, the complex coordinate rotation technique is employed in our calculation. This method will supply complex eigenvalues with their imaginary parts corresponding to the natural linewidth of the absorption. In the case of pure electric fields, the radial wavefunction of the system can be expanded in terms of B-spline basis as

$$R_n(r) = \sum_i C_i^n B_i^k(r), \tag{4}$$

where B_i^k is the i-th B-spline of order k defined in Refs. [39] and [40], while the angular wavefunction is expanded in spherical harmonic functions.

For the calculation of the Stark spectra of barium within an examined energy range, the quantum defects of different channels are determined by sweeping their values as mentioned in our previous paper.[36] We take the "standard values" as follows: $\delta_{\rm s} = 0.29$, $\delta_{\rm p} = 0$, $\delta_{\rm d} = -0.34$ and those for the higher angular momentum states are equal to zero. For our excitation scheme of one-photon irradiation from the ground state $6{\rm s}^2\ {}^1{\rm S}_0$, only $6{\rm snp}\ {}^1{\rm P}_1$ is populated in a free field.

3. Experimental setup

Our experiment is based on the same apparatus introduced previously.[36] We adjust the laser beam to be perpendicular to the atomic beam so that Doppler broadening can be minimized. The Stark plates are aligned with their electric field perpendicular to the atom beam and laser pulse, thus we can measure the π and σ spectrum. A Soleil–Babinet compensator is used to convert the laser from horizontal polarization to vertical, and we can obtain the π polarized spectra with $\Delta M = 0$. The pulsed laser used in our experiment is generated by an Yttrium Aluminum Garnet pumped Lambda Physik Scanmate 2E dye laser system with a linewidth of 0.15 cm^{-1}. The laser beam from the dye laser is frequency doubled by a BBO crystal and the dichromatic beams are separated by two pairs of prisms. The atomic beam is produced by a home-made oven heated to 700 °C with a pinhole diameter of 1 mm. Highly excited atoms emerging from the interaction region travel 7 mm before entering the electric field ionization region. The ionized atoms travel 30 cm in a shielded tube and finally arrive at the multichannel plates (MCPs) located at the end of interaction chamber. The ionic signal from the MCPs is recorded by a data acquisition card and their time of flight is registered. Spectra are obtained by monitoring the integrated TOF signal as a function of laser wave number.

The inhomogeneous electric field was generated by applying constant voltages to the two Stark plates separated by 5 mm and keeping the ionization grid on the excitation side grounded. The atoms will fly out from high-field region towards zero field after excitation and then be ionized. Due to the presence of a negative gradient electric field, the atoms with Stark states $k > 0$ ($k < 0$) are subject to an accelerating (decelerating) force.

4. Results and discussion

The Stark maps of barium in the two energy ranges of $-94 \sim 85$ cm^{-1} and $-115 \sim 106$ cm^{-1} are presented in Figs. 1 and 2, respectively. When the excited atoms fly out of the Stark plates, the electric fields will decrease to zero and there exists a natural electric field gradient during the escaping passage. At the same time, the electric field will induce a dipole moment for the atom. In this gradient field, the excited barium atom with a non-zero dipole moment will interact with the electric field. The direction of force imposed on the atoms is closely

related to the gradient direction and the dipole moment sign. If the force is in the same direction as the flying direction, the atom will accelerate. On the contrary, the atom will decelerate. This effect can be revealed by the time of flight spectrum of the specified states as shown in Figs. 3 and 4, corresponding to the Stark maps in Figs. 1 and 2.

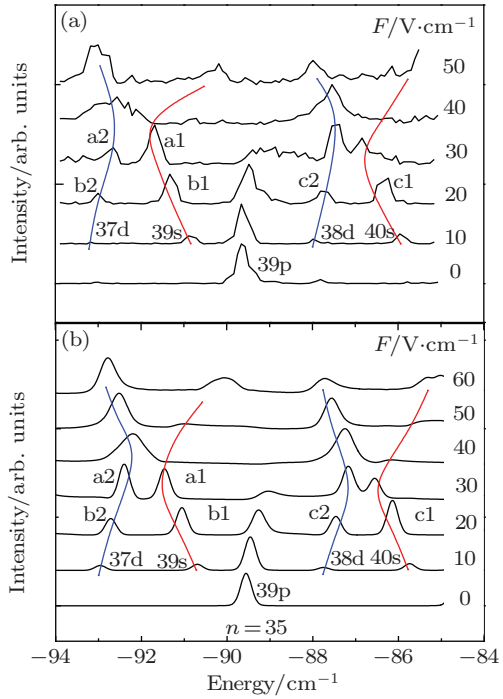


Fig. 1. (color online) (a) Experimental and (b) theoretical Stark maps of barium over an energy range of -94 cm^{-1} to -85 cm^{-1} with $m=0$ and $n=35$. The anti-crossings in experiments are observed and identified with the help of the theoretical calculation.

We firstly look at the experimental Stark map of barium in the energy range -94 cm^{-1} to -85 cm^{-1} shown in Fig. 1(a). In the examined energy range, only 39p is populated at free field, and the quantum defect of p state is nearly integer. As the electric field increases, the p state will instantly interact with the hydrogen-like states (with small quantum defect) and then s and d states by coupling. The competition between these interactions determines the final line positions and intensities of the Stark states. In our case, the p dominant manifold shifts to high energy slightly with the electric field. At higher electric field, for example, at $F=30$ V·cm^{-1}, the p dominant peak passes much of its spectral intensity to s and d states by coupling and itself gets very weak. Beyond this electric field value, this spectral line disappears completely.

This interaction can also occur between the states from different principal quantum numbers n. When the electric field comes to 40 V·cm^{-1}, 37d and 39s states approach closely but repel each other. At this moment, an anti-crossing occurs. The core-induced interaction between the neighboring n-manifolds accounts for the anti-crossings. The same situation happens to 38d and 40s states. These anti-crossings make the spectrum very complex. For the Stark map in the energy range of -115 cm^{-1} to -106 cm^{-1}, the case is similar to the anti-crossing which occurs at the higher electric field, i.e., $F=60$ V·cm^{-1}, which is clarified in Fig. 2.

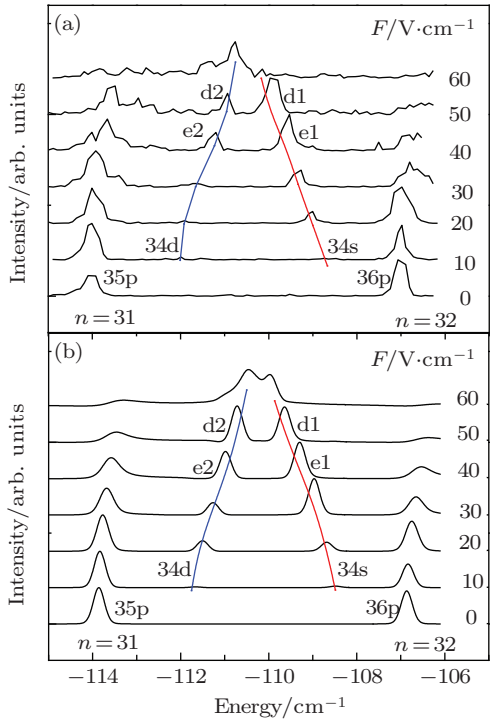


Fig. 2. (color online) (a) Experimental and (b) theoretical Stark maps of barium in an energy range of -115 cm^{-1} to -106 cm^{-1} with $m=0$. The anti-crossings in experiments are observed and identified with the help of theoretical calculations.

To understand these anti-crossings, we make a calculation and reproduce the Stark maps at corresponding energy ranges. The calculated spectra are shown in Figs. 1(b) and 2(b). In the calculation, the quantum defect "standard values" mentioned in the theory part are employed. It can been seen that the calculated spectra agree with the experiments very well.

As discussed previously, the polarized atom in an electric field will feel a force if the applied electric field is gradient. For a given gradient geometric configuration, it depends on the induced dipole moment of the atom. In our case, the atoms fly out from the Stark plates and this natural scheme presents a negative gradient electric field. For simplifying the discussion, we confine our investigation to the states below the anti-crossing points. Returning to the Stark map shown in Fig. 1, we can expect that the states labeled by a1, b1, and c1 will have opposite mechanical dynamics in the gradient fields compared with those states a2, b2, and c2 since they have opposite dipole moments. Taking state a1 as an instant, the atom prepared in this excited state will absorb energy adiabatically when it flies out of the Stark plates. This feature can be observed in Figs. 1(a) and 1(b). From the point view of energy conservation, the kinetic energy of the atom will reduce, compensated by the quantum state energy increasing. Therefore, the atom will suffer a deceleration. On the contrary, the atom of state a2 will accelerate when it flies out from the Stark electric field. This opposite effect can be observed by comparing

the time of flight spectra as shown by curves I in Fig. 3. We can perform the same analysis for other pairs of states, including those states shown in Fig. 2. The TOF spectra are shown in Figs. 3 and 4.

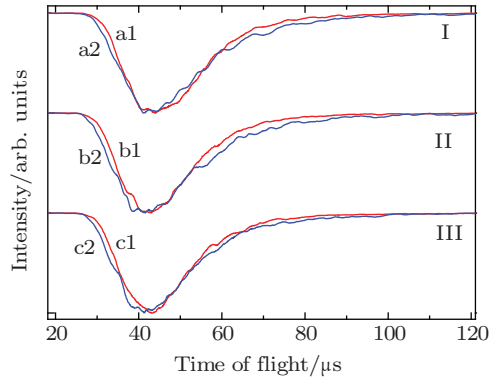


Fig. 3. (color online) Time of flight spectra of the Stark states specified in the Stark map in Fig. 1. The three groups of time of flight spectra correspond to the three pairs of interacting states labeled in Fig. 1, respectively

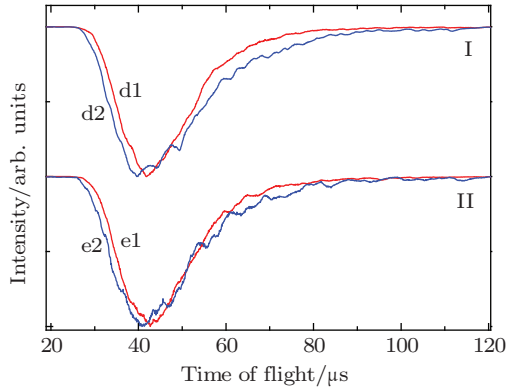


Fig. 4. (color online) Time of flight spectra of the Stark states specified in the Stark map in Fig. 2. The two groups of time of flight spectra correspond to the two pairs of interacting states labeled in Fig. 2, respectively.

It should be noted that the profiles of the time of flight spectra have a long tail due to the large capacitor used in our acquisition circuits. Therefore only the falling edge, i.e., the rising intensity can reflect the time information reliably. We also notice that the time difference is too small, indicating that the acceleration or deceleration effects are not significant. This is due to the small gradient in our experiment where a natural gradient is used. The acceleration and deceleration effect are exaggerated immediately if a violent gradient electric field is applied, which is proved in the processing work in our group.

5. Conclusion

In this paper, we studied the π-polarized Stark spectra of barium at high energies around $n = 35$ experimentally. Calculations are performed to reproduce the observation spectra and the results are satisfying. Coupling between p states and other angular moment states is analyzed in detail in Stark spectra. A fine structure on the anti-crossing of the interacting channels is determined by recording the Stark maps from $F = 0$ to $F = 60$ V·cm^{-1}. Based on the Stark maps, deceleration, and acceleration of barium atoms at specified states are identified.

References

[1] Rojansky V 1929 *Phys. Rev.* **33** 1
[2] Ciocca M, Burkhardt C E, Leventhal J J and Bergeman T 1992 *Phys. Rev.* A **45** 4720
[3] Fabre C, Kaluzny Y, Calabrese R, Liang J, Goy P and Haroche S 1984 *J. Phys.* B **17** 3217
[4] Lahaye C T W, Hogervorst W and van der Veldt T 1989 *Z. Phys.* D **13** 107
[5] Courtney M, Spellmeyer N, Jiao H and Kleppner D 1995 *Phys. Rev.* A **51** 3604
[6] Wang L, Quan W, Shen L, Yang H F, Shi T Y, Liu X J, Liu H P and Zhan M S 2009 *Chin. Phys.* B **18** 4791
[7] Ito K, Masuda H, Morioka Y and Ueda K 1993 *Phys. Rev.* A **47** 1187
[8] Littman M G, Zimmerman M L, Ducas T W, Freeman R R and Kleppner D 1976 *Phys. Rev. Lett.* **36** 788
[9] Freeman R R, Economou N P, Bjorklund G C and Lu K T 1978 *Phys. Rev. Lett.* **41** 1463
[10] Freeman R R and Economou N P 1979 *Phys. Rev. A.* **20** 2356
[11] Sandner W, Safinya K A and Gallagher T F 1981 *Phys. Rev.* A **23** 2448
[12] Ducas T W, Littman M G, Freeman R R and Kleppner D 1975 *Phys. Rev. Lett.* **35** 366
[13] Littman M G, Kash M M and Kleppner D 1978 *Phys. Rev. Lett.* **41** 103
[14] Rice M H and Good R H 1962 *J. Opt. Soc. Am.* **52** 239
[15] Zimmerman M L, Littman M G, Kash M M and Kleppner D 1979 *Phys. Rev.* A **20** 2251
[16] Lahaye C T W, Hogervorst W and Vassen W 1987 *Z. Phys.* D **7** 37
[17] Zimmerman M L, Ducas T W, Littman M G and Kleppner D 1978 *J. Phys.* B **11** L11
[18] Jiang T, Bowden M D, Wagenaars E, Stoffels E and Kroesen G M W 2006 *J. Phys.* D **39** 5216
[19] Sakimoto K 1986 *J. Phys.* B **19** 3011
[20] Zhi M c, Dai C j and Li S B 2001 *Chin. Phys.* **10** 929
[21] Seipp I and Taylor K T 1994 *J. Phys.* B **27** 2785
[22] Simons G 1974 *J. Chem. Phys.* **60** 645
[23] Menéndez J M, Martín I and Velasco A M 2005 *Int. J. Quantum. Chem.* **102** 956
[24] Breeden T and Metcalf H 1981 *Phys. Rev. Lett.* **47** 1726
[25] Procter S R, Yamakita Y, Merkt F and Softley T P 2003 *Chem. Phys. Lett.* **374** 667
[26] Townsend D, Goodgame A L, Procter S R, Mackenzie S R and Softley T P 2001 *J. Phys.* B **34** 439
[27] Yamakita Y, Procter S R, Goodgame A L, Softley T P and Merkt F 2004 *J. Chem. Phys.* **121** 1419
[28] Bethlem H L, Berden G and Meijer G 1999 *Phys. Rev. Lett.* **83** 1558
[29] Bethlem H L, Crompvoets F M H, Jongma R T, van de Meerakker S Y T and Meijer G 2002 *Phys. Rev.* A **65** 053416
[30] van de Meerakker S Y T, Vanhaecke N and Meijer G 2006 *Annu. Rev. Phys. Chem.* **57** 159
[31] Vliegen E and Merkt F 2006 *J. Phys.* B **39** L241
[32] Vliegen E, Worner H J, Softley T P and Merkt F 2004 *Phys. Rev. Lett.* **92** 033005
[33] Hogan S D and Merkt F 2008 *Phys. Rev. Lett.* **100** 043001
[34] Vliegen E, Hogan S D, Schmutz H and Merkt F 2007 *Phys. Rev.* A **76** 023405
[35] Liu H P, Quan W, Shen L, Connerade J P and Zhan M S 2007 *Phys. Rev.* A **76** 013412
[36] Yang H F, Gao W, Quan W, Liu X J and Liu H P 2012 *Phys. Rev.* A **85** 032508
[37] Hu Z F, Zhao H T, Zhou S K, Gong S S and Zhan M S 2000 *Chin. Phys.* **9** 805
[38] Menéndez J M, Martín I and Velasco A M 2004 *Chem. Phys. Lett.* **398** 287
[39] Bachau H, Cormier E, Decleva P, Hansen J E and Martín F 2001 *Rep. Prog. Phys.* **64** 1815
[40] de Boor C 1972 *J. Approx. Theory* **6** 50